





Article

# Double *K*-Shell Ionization of Ar by 197-MeV/u Xe<sup>54+</sup> Ion Impact

Caojie Shao <sup>1,2,\*</sup> , Deyang Yu <sup>1,2</sup>, Yury S. Kozhedub <sup>3</sup> , Kun Ma <sup>4</sup>, Zhangyong Song <sup>1,2</sup> , Wei Wang <sup>1,2</sup>, Yingli Xue <sup>1,2</sup>, Mingwu Zhang <sup>1,2</sup> , Junliang Liu <sup>1,2</sup>, Bian Yang <sup>1,2</sup>, Chenzhong Dong <sup>5</sup>, Hongqiang Zhang <sup>6</sup> and Xiaohong Cai <sup>1,2</sup>

<sup>1</sup> Institute of Modern Physics, Chinese Academy of Sciences, Lanzhou 730000, China  
<sup>2</sup> University of Chinese Academy of Sciences, Beijing 100049, China  
<sup>3</sup> Department of Physics, St. Petersburg State University, St. Petersburg 198504, Russia  
<sup>4</sup> School of Information Engineering, Huangshan University, Huangshan 245041, China  
<sup>5</sup> College of Physics and Electronic Engineering, Northwest Normal University, Lanzhou 730070, China  
<sup>6</sup> School of Nuclear Science and Technology, Lanzhou University, Lanzhou 730000, China  
\* Correspondence: c.shao@impcas.ac.cn

**Abstract:** We present an experimental study on the double *K*-shell ionization of argon in single collisions with the Xe<sup>54+</sup> ion at 197 MeV/u. The X-ray spectra of multi-ionized argon are measured at the observation angles of 90° and 145° with respect to the projectile beam. The target *K* X-ray satellite and hypersatellite lines are analyzed with a fitting model and the cross-section ratio of double to single *K*-shell ionization is derived. The experimental results are compared to the relativistic time-dependent, two-center calculations, and a reasonable agreement is reached.

**Keywords:** double *K*-shell ionization; heavy ion; X-ray emission; *K*-shell hollow atom



**Citation:** Shao, C.; Yu, D.; Kozhedub, Y.S.; Ma, K.; Song, Z.; Wang, W.; Xue, Y.; Zhang, M.; Liu, J.; Yang, B.; et al. Double *K*-Shell Ionization of Ar by 197-MeV/u Xe<sup>54+</sup> Ion Impact. *Atoms* **2022**, *10*, 155. <https://doi.org/10.3390/atoms10040155>

Academic Editor: Jean-Christophe Pain

Received: 17 November 2022

Accepted: 15 December 2022

Published: 19 December 2022

**Publisher's Note:** MDPI stays neutral with regard to jurisdictional claims in published maps and institutional affiliations.



**Copyright:** © 2022 by the authors. Licensee MDPI, Basel, Switzerland. This article is an open access article distributed under the terms and conditions of the Creative Commons Attribution (CC BY) license (<https://creativecommons.org/licenses/by/4.0/>).

## 1. Introduction

The double *K*-shell ionization of atoms by the impact of charged ions is one of typical two-electron processes considerably studied by theories and experiments [1–5]. The double *K*-shell ionization of heavy atoms can also provide the possibilities to investigate exotic decay modes, such as hypersatellite transitions [6–9], the hypersatellite Auger process [10,11], two-electron one-photon (TEOP) transitions [12], and the three-electron Auger process [13]. Experiments on these decay processes can be accessed in the collisions of energetic heavy ions, in particular bare ions, with target atoms, where the strong Coulomb field of the projectile causes the simultaneous ejection of the two *K*-shell electrons of the target atoms with a significant cross-section [14,15].

The production of double *K*-shell vacancies in heavy atoms by bare heavy ions with energies ranging from several to tens of MeV/u has been widely studied in the last decades [4,16–19]. By measuring and analyzing the *K* X-ray spectrum, Hall et al. studied the formation mechanism of double *K*-shell vacancies in titanium atoms in the collision with 5–15-MeV/u Cl<sup>17+</sup> [4,16], 2.0–6.0 MeV/u Si<sup>14+</sup> [16], 5 MeV/u F<sup>9+</sup>, Mg<sup>12+</sup>, and Al<sup>13+</sup> ions [16], respectively. Experimental studies of such a process for argon were also carried out with gaseous targets by Schulz et al. and by Wohrer et al. by employing 0.5 MeV/u S<sup>16+</sup> [17] and 7.0 MeV/u Fe<sup>26+</sup> beams [18], respectively. More recently, Hillenbrand et al. presented a study of double *K*-shell vacancies in xenon atoms in symmetric collisions with 15–50-MeV/u Xe<sup>54+</sup> ions [19]. In these cases, the ion velocity  $v_p$  is lower than or close to the classical velocity of the target atomic electron  $v_K$ ; the formation mechanisms of double *K*-shell vacancies in atoms are complicated, due to the contributions of the direct ionization and electron transfer, while the situation gets simpler when  $v_p$  is far greater than  $v_K$ . The two *K*-shell electrons of the target atom are considered to be removed dominantly by two independent direct single-ionization events [14]. The experimental study of this process is important for mapping the limits of the applicability of the independent electron approximation, which is usually considered to be valid for multiple inner-shell ionization.

This requires the relativistic energies for the incident heavy ions according to the classical velocity of the  $K$ -shell electrons for atoms with the medium atomic numbers ( $Z$ ). However, the availability of the relativistic heavy ions made these studies scarce.

Heavy-ion storage rings, characterized by relativistic energies and high- $Z$  bare ions, combined with gaseous internal targets, provide new possibilities for the investigations of the special atoms/ions with the double  $K$ -shell vacancies with a wide variety of ion species and energies. In addition, environmental effects during the collision and decay processes, such as secondary ionization and interatomic transition, can be suppressed effectively in gas target experiments [8]. In a previous experiment, we studied the dynamic formation of double  $K$ -shell vacancies in krypton atoms in collisions with 52–197-MeV/u  $\text{Xe}^{54+}$  ions through the X-ray spectroscopy method at a heavy-ion storage ring equipped with an internal gas-jet target, where the corresponding  $v_p/v_K$  ranges from 1.2 to 2.2 [15]. In this paper, we report the results of an X-ray spectroscopy study of the argon atoms with the double  $K$ -shell vacancies produced in single collisions with relativistic (197-MeV/u) bare xenon ions. The present work is a continuation of our previous study, and its main goal is to explore the creation of  $K$ - and  $L$ -shell vacancies in argon atoms colliding with heavy bare ions in the higher  $v_p/v_K$  region, as well as the filling processes of the  $K$ -shell vacancies. The experiment and data analysis methods are described in the second and third sections, respectively. The results and discussions are presented in Section 4, and finally, a conclusion of the present work and a brief outlook are given in Section 5.

## 2. Experiment

The measurement was carried out at the HIRFL-CSR (Heavy Ion Research Facility at Lanzhou–Cooling Storage Ring) with its internal target [20,21]. The details of the experiment have been described elsewhere [15]. Briefly, a beam bunch of about  $10^7$   $\text{Xe}^{54+}$  ions with the energy of 197 MeV/u was injected into the experimental ring (CSRe); it was cooled by the electron cooler and then collided with the argon gas-jet target. The beam current was about 100–600  $\mu\text{A}$ , and the target thickness was around  $10^{12}$ – $10^{13}$  atoms/cm<sup>2</sup> during the measurement. The beam energy loss, due to the interaction with the target, was compensated by the continuous electron cooling. The projectile ions that capture one electron were separated from the circulating beam due to the change in their magnetic stiffness.

The X-rays produced in the collisions of the ions with the target were registered by a lithium-drifted silicon [Si(Li)] detector mounted at 90° and a high-purity germanium (HPGe) detector at a 145° observation angle with respect to the ion beam direction. The distances between the detectors and the interaction point were 270 and 500 mm, respectively. The detectors were isolated from the ultrahigh vacuum system of the interaction chamber by 100  $\mu\text{m}$  beryllium windows, shielded by lead and brass assemblies and collimated by holes of an 8 mm diameter. The detectors were calibrated using radioactive sources of <sup>55</sup>Fe, <sup>133</sup>Ba, <sup>152</sup>Eu, and <sup>241</sup>Am before and after the experiments. The energy resolutions (i.e., full width at half maximum) of the present detectors are both about 181 eV at around 3.0 keV.

## 3. Data Analysis Methods

### 3.1. Spectra Fitting of $K$ X-ray

The spectrum of argon  $K$  X-rays recorded by the Si(Li) detector are shown in Figure 1. The weight center positions of the argon  $K\alpha$  and  $K\beta$  diagram transitions,  $K\alpha^d$  and  $K\beta^d$ , at 2.957 keV and 3.191 keV, are indicated by the vertical lines, respectively [22]. The clear shift of the experimental peaks to higher energies indicates high ionizations of the argon atoms. The energy intervals between the  $K\alpha^s$ ,  $K\alpha^{h,s}$ ,  $K\beta^s$ , and  $K\beta^{h,s}$  peaks are close to the resolution of the detectors ( $\sim 180$  eV) [23]. The origin of the  $K\alpha^s$ ,  $K\beta^s$  satellite and  $K\alpha^{h,s}$ ,  $K\beta^{h,s}$  hypersatellite peaks is described in detail in our previous paper [15]. The  $K\alpha^s$ ,  $K\beta^s$  satellite and  $K\alpha^{h,s}$ ,  $K\beta^{h,s}$  hypersatellite peaks come from the transitions of the following types:  $K^{-1}L^{-n_L}M^{-n_M} \rightarrow K^0L^{-(n_L+1)}M^{-n_M}$ ,  $K^{-1}L^{-n_L}M^{-n_M} \rightarrow K^0L^{-n_L}M^{-(n_M+1)}$ ,  $K^{-2}L^{-n_L}M^{-n_M} \rightarrow K^{-1}L^{-(n_L+1)}M^{-n_M}$ , and  $K^{-2}L^{-n_L}M^{-n_M} \rightarrow K^{-1}L^{-n_L}M^{-(n_M+1)}$ , respectively.

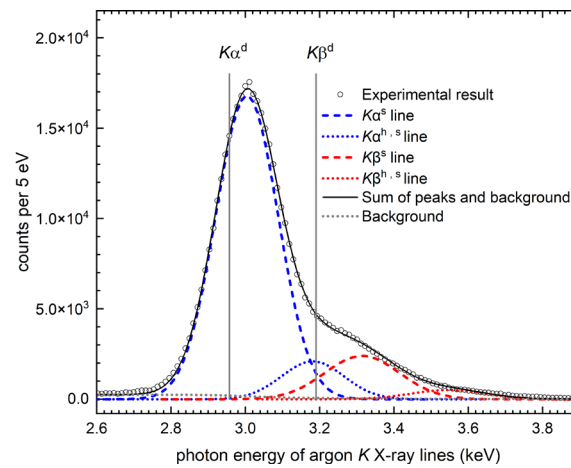


**Figure 1.** Measured spectra of X-rays emitted from argon target in the collisions with 197-MeV/u  $\text{Xe}^{54+}$  ions, obtained by the Si(Li) detector at the  $90^\circ$  observation angle. The measured data are represented by open circles, while the fitted transitions are represented by dashed curves. The fitted background is shown as gray dotted line.

All the four peaks contain the X-rays emitted from states with different  $L$ -shell and  $M$ -shell vacancies, resulting in broadened Gaussian profiles. By only using the energies and widths of the peaks as free-fitting parameters, those peaks can be fitted unambiguously. In this case, we adopt an approach similar to that developed by D. Banas et al. [24]. As the mean number of  $L$ -vacancies,  $n_L^x$ , is very close when a hypersatellite and satellite transition occurs [8], we further simplify the correlation of the fitting parameters here. The  $K\alpha^s$ ,  $K\alpha^{h,s}$ ,  $K\beta^s$ , and  $K\beta^{h,s}$  peaks are fitted by four Gaussian distributions with the following parameters: (a) the positions of these four peaks are all expressed in terms of the mean  $L$ -vacancy number  $n_L^x$  at the time of X-ray emission; (b) the full widths at half maximum (FWHM) of the  $K\alpha^s$  and  $K\alpha^{h,s}$  peaks are set to the same because of the identical peak widths of  $K\alpha^s$  and  $K\alpha^{h,s}$  for the same  $n_L^x$ , as derived by convolution and fitting [23]; so, the same occurred for the  $K\beta^s$  and  $K\beta^{h,s}$  peaks for the same reason. Therefore, a total of seven parameters (four peak intensities, two peak widths, and  $n_L^x$ ) are used.

The transition energies and decay rates of argon  $K\alpha^s$ ,  $K\alpha^{h,s}$ ,  $K\beta^s$ , and  $K\beta^{h,s}$  as a function of the vacancy number in the  $L$ -shell were calculated using the GRASP 2K program [25]. The energy shifts caused by  $M$ -shell vacancies are assumed to be proportional to their number and given by the difference between the calculated results when the  $M$ -shell is full and when there is only one  $M$ -vacancy. The binomial population distributions of the number of the  $L$ - and  $M$ -shell vacancies in the target atoms at the time of the  $K$ -shell radiations are assumed [26]. The average numbers of  $L$ -vacancy  $n_L^x$  and  $M$ -vacancy  $n_M^x$  were associated by a scaling formula [27]. The results were the convolutions of the population distributions of the number of the  $L$ - and  $M$ -shell vacancies and Gaussians for a detector resolution of 181 eV. The weight center energies of the  $K^{-1}L^0 \rightarrow K^0L^{-1}$  and  $K^{-1}L^0M^0 \rightarrow K^0L^0M^{-1}$  argon transitions are calculated to be 3.131 and 3.1416 keV, respectively. The mean energy of  $K\alpha^s$ ,  $K\alpha^{h,s}$ ,  $K\beta^s$ , and  $K\beta^{h,s}$  as a function of the spectator  $L$ -vacancy number  $n_L^x$  are obtained as follows:

$$E_{K\alpha^s} = 2.957 + 0.0192n_L^x \quad (1)$$

$$E_{K\alpha^{h,s}} = 3.131 + 0.0198n_L^x \quad (2)$$

$$E_{K\beta^s} = 3.191 + 0.0495n_L^x \quad (3)$$

$$E_{K\beta^{h,s}} = 3.416 + 0.0516n_L^x \quad (4)$$

The Gaussian fittings of the experimental X-ray spectra were carried out after the correction of the detection efficiency and subtraction of the linear background. Figure 1 depicts the fitting curves as well. The energies, widths, relative intensities of the peaks, and

spectator  $L$ -vacancy numbers are listed in Table 1. The energy uncertainties include the detector calibration error and the fitting error. The former contributes  $\pm 3$  eV as evaluated from measuring the argon  $K\alpha$  diagram lines by an X-tube. The total uncertainties in the energy shift are estimated to be within  $\pm 5$  eV, resulting in an 0.3 uncertainty for  $n_L^x$ .

**Table 1.** The determined relative intensities  $I(K\alpha^{h,s})/I(K\alpha^s)$ , the energy, and FWHM of  $K\alpha^s$ ,  $K\alpha^{h,s}$ ,  $K\beta^s$  and  $K\beta^{h,s}$  peaks, as well as the average number of spectator  $L$ -vacancies  $n_L^x$  of argon in collision with 197-MeV/u Xe<sup>54+</sup> ion. The data include measurements at both the Si(Li) at the 90° observation angle and the germanium detectors at the 145° observation angle.

Results	Detection Angle of 90°	Detection Angle of 145°
$I(K\alpha^{h,s})/I(K\alpha^s)$	$0.107 \pm 0.02$	$0.119 \pm 0.02$
$E(K\alpha^s)/FWHM$ (keV)	$3.0007/0.199$	$3.0037/0.206$
$E(K\alpha^{h,s})/FWHM$ (keV)	$3.1778/0.199$	$3.1808/0.206$
$E(K\beta^s)/FWHM$ (keV)	$3.3058/0.238$	$3.3132/0.244$
$E(K\beta^{h,s})/FWHM$ (keV)	$3.5371/0.238$	$3.5448/0.244$
$n_L^x$	$2.34 \pm 0.3$	$2.49 \pm 0.3$

It can be seen from Table 1 that all of the deduced results from the spectrum at 90° are consistent with those from 145°. The  $K\beta^s$  and  $K\beta^{h,s}$  peaks shift much more than the  $K\alpha^s$  and  $K\alpha^{h,s}$  peaks. In addition, the Gaussian profiles of the  $K\beta^s$  and  $K\beta^{h,s}$  peaks broadened more than the  $K\alpha^s$  and  $K\alpha^{h,s}$  peaks. This is due to the fact that the  $L$ -vacancies affect the transitions from the upper  $M$ -shell more than those from the  $L$ -shell.

### 3.2. Fluorescence Yields of Argon with Multiple Vacancy

In order to deduce the ratio of the double to single  $K$ -shell ionization cross-section of argon atoms from the relative intensities of emitted  $K\alpha^{h,s}$  and  $K\alpha^s$  X-rays, the fluorescence yields of argon with multiple vacancies are required. The fluorescence yields  $\omega_{K\alpha^{h,s}}$  and  $\omega_{K\alpha^s}$  for argon with different spectator vacancies in the  $K$ -shell,  $L$ -shell, and  $M$ -shell should be undertaken for each parent defect configuration and are currently not available. Therefore, the fluorescence yields of multivacancy configurations are derived using a statistical weighting procedure developed by Larkins [28]. The original radiative and radiationless transition rates of a single  $K$  vacancy are obtained from the tabulated data [29,30]. The relationship between the initial vacancy distribution of argon atoms by projectile impacts and their time evolutions by taking into account multi-step vacancy rearrangement processes is evaluated by the model developed by Horvat et al. [31]. The population distributions of the number of target atom  $L$ - and  $M$ -shell vacancies from collisions are also assumed to be binomial. According to the scaling formula, the average numbers of the spectator  $L$ -vacancy  $n_L^0$  and  $M$ -vacancy  $n_M^0$  are associated [27].

The relationship between  $n_L^x$  and  $n_L^0$  with and without considering the vacancy rearrangement process, is shown in Figure 2a. In the figure, the experimental data are also shown (denoted by horizontal and vertical dashed lines). The experimental  $n_L^x$  is obtained by averaging the data at the observation angles (90° and 145°). It can be seen that  $n_L^x$  is significantly smaller in the case which considers vacancy rearrangement than the case which does not consider vacancy rearrangement. This means that a part of the  $L$ -vacancies is filled by electrons in higher levels before the  $K$  X-ray emission during the vacancy rearrangement process. The  $n_L^x$  for the  $K\alpha^{h,s}$  radiation is larger than that for the  $K\alpha^s$  radiation if they have the same initial  $n_L^0$ . This is due to the fact that the  $K$ -shell is filled faster for the double  $K$ -vacancies than for the single  $K$ -vacancy.

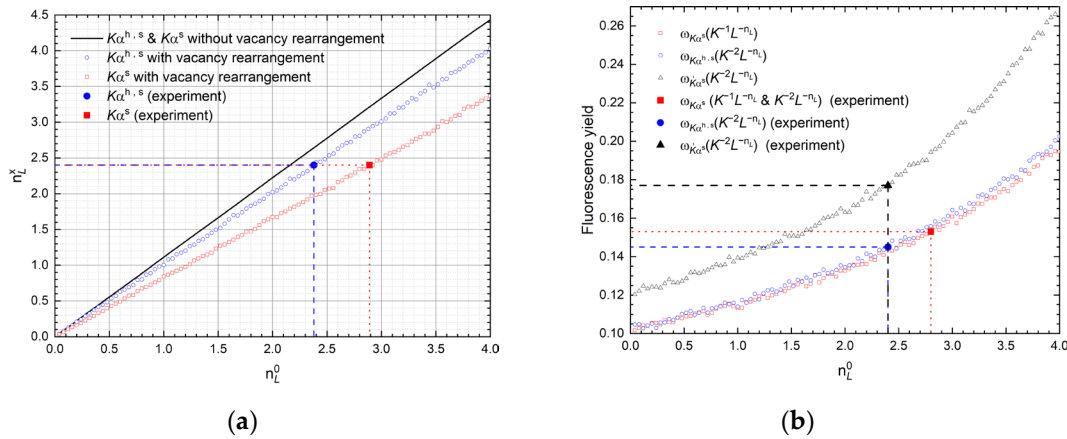


**Figure 2.** (a) Calculated average numbers of spectator  $L$ -shells at the time of X-ray emission  $n_L^x$  versus that of spectator  $L$ -shells produced in the collision  $n_L^0$  for argon. (b) The calculated fluorescence yields  $\omega_{K\alpha^s}$ ,  $\omega_{K\alpha^{h,s}}$  and  $\omega'_{K\alpha^s}$  versus  $n_L^0$  for argon. The experimental results are represented by solid symbols with vertical and horizontal lines indicating their coordinates.

Accordingly, the average fluorescence yields of the  $K\alpha^{h,s}$  from the  $K^{-2}L^{-n_L}$  states  $\omega_{K\alpha^{h,s}}$ , the  $K\alpha^s$  from the  $K^{-1}L^{-n_L}$  states  $\omega_{K\alpha^s}$ , and the  $K\alpha^s$  originating from the cascade decay of the  $K^{-2}L^{-n_L}$  states  $\omega'_{K\alpha^s}$  versus the  $n_L^0$  are shown in Figure 2b, respectively. These three yields all increase as  $n_L^0$  increases. The  $\omega'_{K\alpha^s}$  is significantly larger than the  $\omega_{K\alpha^{h,s}}$  and  $\omega_{K\alpha^s}$  at the same  $n_L^0$ . This is because the number of vacancies in the  $L$  shell will increase when the first  $K$ -shell vacancy is filled through the dominant  $KL$  radiation or the  $KLM$  and  $KLL$  Auger processes. The experimental  $\omega_{K\alpha^{h,s}}$  and  $\omega'_{K\alpha^s}$  deduced from the  $n_L^0$  of the  $K^{-2}L^{-n_L}$  states, as well as the  $\omega_{K\alpha^s}$  from the  $n_L^0$  of the  $K^{-1}L^{-n_L}$  states, are shown in Figure 2b by the blue and black dashed lines and the red dot horizontal lines, respectively. Their values are 0.145, 0.153, and 0.177, respectively. It should be noted that the measured  $K\alpha^s$  lines contain the  $K\alpha^s$  lines of the  $K^{-1}$  states originating from the cascade decay of the  $K^{-2}L^{-n_L}$  states.

#### 4. Results and Discussion

The cross-section ratio between the double  $\sigma_{K^{-2}}$  and the single  $\sigma_{K^{-1}}$   $K$ -shell ionization can be calculated from

$$\frac{\sigma_{K^{-2}}}{\sigma_{K^{-1}}} = \frac{R_{21}^x}{\omega_{K\alpha^{h,s}}/\omega_{K\alpha^s} - R_{21}^x \omega_{K\alpha^{h,s}}/\omega'_{K\alpha^s}} \quad (5)$$

where  $R_{21}^x$  is the relative intensities  $I(K\alpha^{h,s})/I(K\alpha^s)$ . Taking the relative intensities of the X-ray emission listed in Table 1 and the fluorescence yields deduced in Section 3, the ionization cross-section ratios for argon collided by the 197 MeV/u  $\text{Xe}^{54+}$  ion were obtained and are listed in Table 2. The experimental mean number of the  $L$ -vacancies produced by collision  $n_L^0(K^{-2}L^{-n_L})$  is also shown in in Table 2. The mean number of  $L$ -vacancies of the  $K^{-1}L^{-n_L}$  state in collision  $n_L^0(K^{-1}L^{-n_L})$  is not given here because we do not try to distinguish between the contributions of the  $K^{-1}L^{-n_L}$  states produced in collision and those originating from the cascading of the  $K^{-2}L^{-n_L}$  states under the current experimental resolution.

**Table 2.** Comparison of our experimental results with theory for target single and double  $K$ -shell vacancy production. The uncertainty of intensity ratio comes from the uncertainties of the fitting parameters. The uncertainty of the deduced mean  $L$ -vacancies is estimated by detection error and fitting error.

Projectile	Experiment		Theory (RCC)			
	$\sigma_{K^{-2}}/\sigma_{K^{-1}}$	$n_L^0(K^{-2}L^{-n_L})$	$\sigma_{K^{-2}}$ (kbarn)	$\sigma_{K^{-1}}$ (kbarn)	$\sigma_{K^{-2}}/\sigma_{K^{-1}}$	$n_L^0(K^{-2}L^{-n_L})$
197 MeV/u $\text{Xe}^{54+}$	$0.12 \pm 0.02$	$2.4 \pm 0.3$	289	2709	0.1067	3.56

In the present work, the velocity of ion  $v_p$  is 77.4 a.u, which is about 4.3 times the velocity of the atom’s  $K$ -shell electrons, but the perturbation strength from the projectile ion  $\kappa$  ( $\kappa = Z_p/v_p$ ,  $Z_p$  is the nuclear charge of the projectile) is 0.70, which is close to 1. Thereby the non-perturbative relativistic coupled-channel (RCC) method based on the independent electron model and the two-center atomic-like Dirac–Fock–Sturm orbitals as a basis set are adopted to calculate the cross-sections of single and double  $K$ -shell ionizations [32]. The calculation results are also shown Table 2. The experimental ratio  $R_{21}$  for the double-to-single target  $K$ -shell vacancy production cross-section is slightly greater, but it agrees reasonably with the theoretical result. This indicates that the independent electron approximation is still suitable for the process of  $K$ -shell multiple ionization in the current collision system.

The deduced mean number of spectator  $L$ -vacancies produced when the double  $K$ -shell vacancies created in collision  $n_L^0(K^{-2}L^{-n_L})$  in the experiment is less than the theoretical result. At present, it is difficult to identify conclusively whether the remaining discrepancy originates from inaccuracies in the theoretical description of the process or in the potentially incomplete fitting model we used. However, some factors need to be mentioned, such as that the strong electron correlations may affect the multiple vacancies production in the  $L$ -shell. The shake-off probability of the  $K$ -shell electron is only 0.001%, while that of the  $L$ -shell electrons is nearly 2%, as the result of a sudden vacancy in the  $K$ -shell for the argon atoms [33]. The simultaneous production of two  $K$ -shell vacancies and multiple  $L$ -shell vacancies may lead to the shake-off of the remaining  $L$ -shell electrons with an even higher probability (>2%). In the experiment, the measurements with higher energy resolutions realized by crystal spectrometers or microcalorimeters will enable us to perform more unconstrained identifications of the related processes. For example, by using a crystal spectrometer with an energy resolution better than 8 eV, the  $K$  X-ray hypersatellite lines from excited argon atoms with different spectator  $L$ -shell vacancies can be fully resolved [8]; then, the  $n_L^x(K^{-2}L^{-n_L})$  could be obtained by the weighted averaging of the  $L$ -vacancy numbers of the individual peaks with their relative intensities, rather than by deducing from the energy shifts of the convolutional peaks. The uncertainty of the obtained  $n_L^x(K^{-2}L^{-n_L})$  will be within 0.1.

### 5. Conclusions

The  $K\alpha^s$ ,  $K\alpha^{h,s}$ ,  $K\beta^s$ , and  $K\beta^{h,s}$  X-rays of multiple ionized argon atoms were measured in single collisions of 197-MeV/u  $\text{Xe}^{54+}$  ions with an argon target. The double  $K$ -shell ionization processes of the argon atoms were investigated by means of the intensity ratios  $I(K\alpha^{h,s})/I(K\alpha^s)$  from a fitting model, combined with the evaluation of the fluorescence yields of the multi-vacancy state atoms and the vacancy rearrangement process. The relative yield of the double  $K$ -shell vacancies of the argon atoms with respect to single the  $K$ -shell ionized ones was determined to be 12%. The experimental cross-section ratio shows a reasonable agreement with the calculated value from the relativistic time-dependent two-center theory. However, the mean number of the spectator  $L$ -vacancies extracted from the experiments is a number that is nearly one less than that of the theory. More precise

experiments with high-resolution detectors are expected to provide a more stringent test of the theory.

**Author Contributions:** Conceptualization, C.S. and D.Y.; methodology, C.S.; investigation: C.S., D.Y., Z.S., W.W., Y.X., M.Z., J.L., B.Y., and X.C.; writing—original draft preparation, C.S.; writing—review and editing: C.S., H.Z., and D.Y.; formal analysis: C.S., Y.S.K., K.M., and C.D. All authors have read and agreed to the published version of the manuscript.

**Funding:** This research was funded by the National Nature Science Foundation of China through grant nos. U1732269, 12275328 and 11674333.

**Data Availability Statement:** Not applicable.

**Acknowledgments:** We thank the crew of the accelerator department for their hardworking operation of the HIRFL-CSR complex.

**Conflicts of Interest:** The authors declare no conflict of interest.

## References

1. McGuire, J.H.; Berrah, N.; Bartlett, R.J.; Samson, J.A.; Tanis, J.A.; Cocke, C.L.; Schlachter, A.S. The ratio of cross sections for double to single ionization of helium by high energy photons and charged particles. *J. Phys. B At. Mol. Opt. Phys.* **1995**, *28*, 913–940. [[CrossRef](#)]
2. Awaya, Y.; Katou, T.; Kumagai, H.; Tonuma, T.; Tendow, Y.; Izumo, K.; Hashizume, A.; Takahashi, T.; Hamada, T. Ratio of single K-shell ionization cross section to double K-shell ionization cross section in heavy-ion-atom collisions. *Phys. Lett. A* **1980**, *75*, 478–480. [[CrossRef](#)]
3. Hall, J.; Richard, P.; Gray, T.J.; Jones, K.; Johnson, B.; Gregory, D. Ratios of double to single K-vacancy production in heavy ion-atom collisions. *Phys. Lett. A* **1982**, *75*, 129–132. [[CrossRef](#)]
4. Hall, J.; Richard, P.; Philip, L.P.; Gregory, D.C.; Miller, P.D.; Moak, C.D.; Jones, C.M.; Alton, G.D.; Bridwell, L.B.; Sofield, C.J. Energy systematics of single and double K-shell-vacancy production in titanium bombarded by chlorine ions. *Phys. Rev. A* **1986**, *33*, 914–920. [[CrossRef](#)] [[PubMed](#)]
5. Kobal, M.; Kavčič, M.; Budnar, M.; Dousse, J.C.; Maillard, Y.P.; Mauron, O.; Raboud, P.A.; Tökési, K. Double-K-shell ionization of Mg and Si induced in collisions with C and Ne ions. *Phys. Rev. A* **2004**, *70*, 062720. [[CrossRef](#)]
6. Briand, J.P.; Chevallier, P.; Tavernier, M.; Rozet, J.P. Observation of K Hypersatellites and KL Satellites in the X-ray Spectrum of Doubly K-Ionized Gallium. *Phys. Rev. Lett.* **1971**, *27*, 777–779. [[CrossRef](#)]
7. Watson, R.L.; Horvat, V.; Peng, Y.  $K\alpha$  X-ray satellite and hypersatellite spectra of vanadium metal and oxides excited in heavy-ion collisions. *Phys. Rev. A* **2008**, *78*, 062702. [[CrossRef](#)]
8. Horvat, V.; Watson, R.L.; Peng, Y.  $K\alpha$  satellite and hypersatellite distributions of Ar excited in heavy-ion collisions. *Phys. Rev. A* **2009**, *79*, 012708. [[CrossRef](#)]
9. Maillard, Y.P.; Dousse, J.C.; Hoszowska, J.; Berset, M.; Mauron, O.; Raboud, P.A.; Kavčič, M.; Rzakiewicz, J.; Banaś, D.; Tökési, K. Hypersatellite X-ray decay of 3d hollow-K-shell atoms produced by heavy-ion impact. *Phys. Rev. A* **2018**, *98*, 012705. [[CrossRef](#)]
10. Köhrbrück, R.; Stolterfoht, N.; Schippers, S.; Hustedt, S.; Heiland, W.; Lecler, D.; Kemmler, J.; Bleck-Neuhaus, J. Electron emission following the interaction of highly charged ions with a Pt(110) target. *Phys. Rev. A* **1993**, *48*, 3731–3740. [[CrossRef](#)]
11. Woods, C.W.; Kauffman, R.L.; Jamison, K.A.; Stolterfoht, N.; Richard, P. K-shell Auger-electron hypersatellites of Ne. *Phys. Rev. A* **1975**, *12*, 1393–1398. [[CrossRef](#)]
12. Wölfli, W.; Stoller, C.; Bonani, G.; Suter, M.; Stöckli, M. Two-Electron-One-Photon Transitions in Heavy-Ion Collisions. *Phys. Rev. Lett.* **1975**, *35*, 656–659. [[CrossRef](#)]
13. Folkerts, L.; Das, J.; Bergsma, S.W.; Morgenstern, R. Three-electron Auger processes observed in collisions of bare ions on a metal surface. *Phys. Lett. A* **1992**, *163*, 73–76. [[CrossRef](#)]
14. McGuire, J.H.; Weaver, L. Independent electron approximation for atomic scattering by heavy particles. *Phys. Rev. A* **1977**, *16*, 41–47. [[CrossRef](#)]
15. Shao, C.; Yu, D.; Cai, X.; Chen, X.; Ma, K.; Evslin, J.; Xue, Y.; Wang, W.; Kozhedub, Y.S.; Lu, R.; et al. Production and decay of K-shell hollow krypton in collisions with 52–197-MeV/u bare xenon ions. *Phys. Rev. A* **2017**, *96*, 012708. [[CrossRef](#)]
16. Hall, J.; Richard, P.; Gray, T.J.; Lin, C.D.; Jones, K.; Johnson, B.; Gregory, D. Double K-shell-to-K-shell electron transfer in ion-atom collisions. *Phys. Rev. A* **1981**, *24*, 2416. [[CrossRef](#)]
17. Schulz, M.; Justiniano, E.; Konrad, J.; Schuch, R.; Salin, A. K-shell to K-shell charge transfer in collisions of bare decelerated S ions with Ar. *J. Phys. B At. Mol. Opt. Phys.* **1987**, *20*, 2057–2073. [[CrossRef](#)]
18. Wohrer, K.; Chetioui, A.; Rozet, J.P.; Jolly, A.; Stephan, C. K-K transfer cross sections in near-symmetric Fe<sup>26+</sup> ion-atom collisions at intermediate velocity. *J. Phys. B At. Mol. Opt. Phys.* **1984**, *17*, 1587. [[CrossRef](#)]
19. Hillenbrand, P.M.; Hagmann, S.; Kozhedub, Y.S.; Benis, E.P.; Brandau, C.; Chen, R.J.; Dmytriiev, D.; Forstner, O.; Glorius, J.; Grisenti, R.E.; et al. Single and double K-shell vacancy production in slow Xe<sup>54+,53+</sup>-Xe collisions. *Phys. Rev. A* **2022**, *105*, 022810. [[CrossRef](#)]

20. Xia, J.W.; Zhan, W.L.; Wei, B.W.; Yuan, Y.J.; Song, M.T.; Zhang, W.Z.; Yang, X.D.; Yuan, P.; Gao, D.Q.; Zhao, H.W.; et al. The heavy ion cooler-storage-ring project (HIRFL-CSR) at Lanzhou. *Nucl. Instr. Meth. Phys. Res. Sec. A* **2002**, *488*, 11–25. [[CrossRef](#)]
21. Shao, C.; Lu, R.; Cai, X.; Yu, D.; Ruan, F.; Xue, Y.; Zhang, J.; Torpokov, D.K.; Nikolenko, D. HIRFL-CSR internal cluster target. *Nucl. Instrum. Meth. Sec. B* **2013**, *317*, 617–622. [[CrossRef](#)]
22. Deslattes, R.D.; Kessler, E.G.; Indelicato, P.; de Billy, L.; Lindroth, E.; Anton, J. X-ray transition energies: New approach to a comprehensive evaluation. *Rev. Mod. Phys.* **2003**, *75*, 35–99. [[CrossRef](#)]
23. Ma, K.; Jiao, Z.; Jiang, F.; Ye, J.; Lv, H.; Chen, Z. Theoretical calculation of  $K\alpha$  and  $K\beta$  X-ray satellite and hypersatellite structures for hollow argon atoms. *Acta Phys. Sin.* **2018**, *67*, 173201.
24. Banaś, D.; Pajek, M.; Semaniak, J.; Braziewicz, J.; Kubala-Kukuś, A.; Majewska, U.; Czyżewski, T.; Jaskóła, M.; Kretschmer, W.; Mukoyama, T. Multiple ionization effects in low-resolution X-ray spectra induced by energetic heavy ions. *Nucl. Instrum. Methods Phys. Res. Sec. B* **2002**, *195*, 233–246. [[CrossRef](#)]
25. Jönsson, P.; Gaigalas, G.; Bieroń, J.; Fischer, C.F.; Grant, I.P. New Version: Grasp2k Relativistic Atomic Structure Package. *Comput. Phys. Commun.* **2013**, *184*, 2197–2203. [[CrossRef](#)]
26. Watson, R.L.; Jenson, F.E.; Chiao, T. Z dependence of  $K\alpha$  X-ray satellite structure in heavy-ion—atom collisions. *Phys. Rev. A* **1974**, *10*, 1230–1244. [[CrossRef](#)]
27. Sulik, B.; Kádár, I.; Ricz, S.; Varga, D.; Végh, J.; Hock, G.; Berényi, D. A Simple Theoretical Approach to Multiple Ionization and Its Application for 5.1 and 5.5 MeV/u  $X^{q+}$ -Ne Collisions. *Nucl. Instrum. Methods Phys. Res. Sec. B* **1987**, *28*, 509–518. [[CrossRef](#)]
28. Larkins, F.P. Dependence of Fluorescence Yield on Atomic Configuration. *J. Phys. B At. Mol. Opt. Phys.* **1971**, *4*, L29–L32. [[CrossRef](#)]
29. Scofield, J.H. Relativistic Hartree-Slater Values for K and L X-ray Emission Rates. *At. Data Nucl. Data Tables* **1974**, *14*, 121–137. [[CrossRef](#)]
30. Chen, M.H.; Crasemann, B.; Mark, H. Relativistic Radiationless Transition Probabilities for Atomic K-and L-Shells. *At. Data Nucl. Data Tables* **1979**, *24*, 13–37. [[CrossRef](#)]
31. Horvat, V.; Watson, R.L.; Blackadar, J.M. Target-Atom Inner-Shell Vacancy Distributions Created in Collisions with Heavy Ion Projectiles. *Nucl. Instrum. Methods Phys. Res. Sec. B* **2000**, *170*, 336–346. [[CrossRef](#)]
32. Kozhedub, Y.S.; Shabaev, V.M.; Tupitsyn, I.I.; Gumberidze, A.; Hagmann, S.; Plunien, G.; Stöhlker, T. Relativistic Calculations of X-ray Emission Following a Xe-Bi<sup>83+</sup> Collision. *Phys. Rev. A* **2014**, *90*, 042709. [[CrossRef](#)]
33. Carlson, T.A.; Nestor, C.W. Calculation of Electron Shake-Off Probabilities as the Result of X-ray Photoionization of the Rare Gases. *Phys. Rev. A* **1973**, *8*, 2887–2894. [[CrossRef](#)]